# REPORT DOCUMENTATION PAGE

Form Approved



AD-A227 780

| 1. AGENCY USE ONLY (Leave blank) | 2. REPORT DATE | 3. R |
|---|---|---|
| | 1990 | |

4. TITLE AND SUBTITLE

(see title on reprint)

NWED QAXM

6. AUTHOR(S)

Swenberg et al.

Work Unit No.
00145

7. PERFORMING ORGANIZATION NAME(S) AND ADDRESS(ES)

Armed Forces Radiobiology Research Institute
Defense Nuclear Agency
Bethesda, MD 20889-5145

8. PERFORMING ORGANIZATION REPORT NUMBER

SR90-23

9. SPONSORING/MONITORING AGENCY NAME(S) AND ADDRESS(ES)

Defense Nuclear Agency
Washington, DC 20305

10. SPONSORING/MONITORING AGENCY REPORT NUMBER

11. SUPPLEMENTARY NOTES

12a. DISTRIBUTION/AVAILABILITY STATEMENT

Approved for public release; distribution unlimited.

12b. DISTRIBUTION CODE

13. ABSTRACT (Maximum 200 words)



14. SUBJECT TERMS

15. NUMBER OF PAGES
10

16. PRICE CODE

| 17. SECURITY CLASSIFICATION OF REPORT | 18. SECURITY CLASSIFICATION OF THIS PAGE | SECURITY CLASSIFICATION OF ABSTRACT | 20. LIMITATION OF ABSTRACT |
|---|---|---|---|
| UNCLASSIFIED | UNCLASSIFIED | | |

# Linear Dichroism Characteristics of Ethidium–and Proflavine–Supercoiled DNA Complexes

CHARLES E. SWENBERG,[1] SUSAN E. CARBERRY,[2]* and NICHOLAS E. GEACINTOV[2]

[1]Radiation Biochemistry Department, Armed Forces Radiobiology Research Institute, Bethesda, Maryland 20814, and [2]Chemistry Department and Radiation and Solid State Laboratory, New York University, New York, New York 10003

## SYNOPSIS

A flow linear dichroism technique is utilized to study the unwinding of supercoiled DNA induced by the binding of ethidium bromide (EB) and proflavine (PF) at different ratios $r$ (drug added/DNA base). In the case of either EB or PF bound to linear calf thymus DNA, the reduced linear dichroism signals LD/A (LD: linear dichroism; A: absorbance, both measured at the same wavelength), determined at 258, and 520 or 462 nm (corresponding to contributions predominantly from the partially oriented DNA bases, intercalated EB, or PF, respectively) are nearly independent of drug concentration. In the case of supercoiled DNA, the magnitude of LD/A at 258 nm first increases to a maximum value near $r = 0.04$–$0.05$, and then decreases as $r$ is increased further, mimicking the behavior of the sedimentation coefficients, viscosities, and gel electrophoresis patterns measured by other workers at similar values of $r$. However, LD/A at 520 nm, which is due to DNA-bound EB molecules, is constant within the range of $r$ values of 0.02–0.06 in which the magnitude of LD/A determined at 258 nm due to the DNA bases exhibits a pronounced maximum. In contrast, in the case of PF, the magnitudes of LD/A determined at 258 or 462 nm are characterized by similar dependencies on $r$, both exhibiting pronounced maxima at $r = 0.05$; this parallel behavior is expected according to a simple intercalation model in which the DNA bases and drug molecules are stacked on top of one another, and in which both are oriented to similar extents in the flow gradient. The unexpected differences in the dependencies of $(LD/A)_{258}$ and $(LD/A)_{520}$ on $r$ in the case of EB bound to supercoiled DNA, are attributed to differences in the net overall alignment of the EB molecules and DNA bases in the flow gradient. The magnitude of the LD signal at 258 nm reflects the overall degree of orientation of the supercoiled DNA molecules that, in turn, depends on their hydrodynamic shapes and sizes; the LD signals characterizing the bound EB molecules may reflect this orientation also, as well as the partial alignment of individual DNA segments containing bound EB molecules. The differences in the LD characteristics of the bound PF and EB molecules may be due to subtle differences in the mechanisms of binding, perhaps reflecting differences in the torsional dynamics and local rigidities in superhelical DNA [Wu et al. (1988) *Biochemistry* **27**, 8128–8144] induced by these two different intercalating agents.

## INTRODUCTION

The existence of circular superhelical DNA in both eukaryotic and prokaryotic cells is well documented, and its characteristics have been studied extensively.[1–4] Many drug molecules that form intercalation complexes with DNA, of which ethidium bromide (EB) is a classical example, are known to unwind supercoiled DNA.[5–9] Electron micrographs show that supercoiled DNA is characterized by highly twisted, compact structures, while the relaxed DNA forms are characterized by open and more extended structures.[5,10] A number of different methods, based on differences in the hydrodynamic properties


CCC 0006-3525/90/141735-10 $04.00
**Biopolymers**, Vol. 29, 1735–1744 (1990)

* Present address: Department of Chemistry, Hunter College of the City University of New York, New York, NY 10021.

of supercoiled, partially relaxed, and relaxed DNA, have been employed to characterize the degrees of unwinding induced by drug molecules. These methods include gel electrophoresis,[9,11] sedimentation velocity,[5-8] and viscometry.[12,13]

We have recently shown[14] that supercoiled DNA can be oriented in the flow gradient of a Couette cell[15] and that changes in superhelicities induced by polycyclic aromatic drugs or carcinogens can also be monitored by linear dichroism (LD) methods. There are several advantages inherent in the LD technique for studying the unwinding and rewinding of supercoiled DNA induced by exogeneous chemicals: (1) the kinetics of unwinding or rewinding of the DNA molecules on time scales of seconds can be followed[14] by monitoring the LD signal within the DNA absorption band (< 300 nm), and (2) the LD signal can be scanned as a function of wavelength; thus, the orientation of the drug molecules causing the changes in superhelicity can be followed by monitoring the LD signal within the wavelength range of the absorption spectrum of the drug.

In this work, we explore the relationships between the LD signals (and thus the relative orientations) of the supercoiled DNA, and of two typical drug molecules, EB and proflavine (PF) (Figure 1), which cause unwinding of the DNA by an intercalation mechanism. In the case of linear calf thymus DNA, the reduced LD within the absorption bands of the DNA and the drugs is approximately the same and independent of the drug concentration. However, in the case of EB–supercoiled DNA complexes, the LD/A ratios within the DNA and drug absorption bands exhibit different dependences on the drug concentrations; this apparent anomaly, which is not apparent in the case of PF–$\phi$X 174 complexes, is attributed to differences in the degrees of alignment in the hydrodynamic flow gradient of the supercoiled DNA molecules as a whole, and of individual linear DNA segments containing the bound EB molecules.

## MATERIALS AND METHODS

The supercoiled DNA samples ($\phi$X 174, SV 40, and pBR322) were purchased from Bethesda Research Laboratories (Bethesda, MD); Topoisomerase I was obtained from Applied Genetics (Freeport, NY), while EB and PF were purchased from Sigma Chemical Co. (St. Louis, MO). Calf thymus DNA (Worthington Biochemicals, Freehold, NJ) was prepared and sonicated as previously described;[16] a reduction in the average molecular weight of the DNA molecules by sonication is desirable, since the average chain length of high molecular weight native DNA is reduced in the hydrodynamic flow field in the Couette cell, thus leading to diminishing LD signals as a function of time. The purity of the supercoiled DNA samples was checked by agarose gel electrophoresis. Completely relaxed marker DNA was obtained by incubating the DNA with Topoisomerase I (1 unit/0.5 $\mu$g DNA, incubation time 30 m at 37°C). Gel electrophoresis was performed using vertical gel slabs (3 mm thick) of 1% agarose (w/v) in TEA buffer (40 m*M* Tris base, 5 m*M* sodium acetate, 1 m*M* EDTA, pH 8.2, 24°C). The gels were stained with EB, photographed under uv light, and the bands were quantitated by densitometry scanning. All samples contained more than 70% of the supercoiled form I DNA.

The flow LD experiments were performed using a Couette cell consisting of a stationary outer cylinder and a rotating inner cylinder, with the DNA solution placed in the annular gap between the two cylinders. The LD signal is defined as follows:

$$LD = A_{\parallel} - A_{\perp} \qquad (1)$$

In these LD measurements, the propagation direction of a linearly polarized light beam is perpendicular to the axis of rotation and parallel to the flow gradient; the LD signal is equal to the difference in

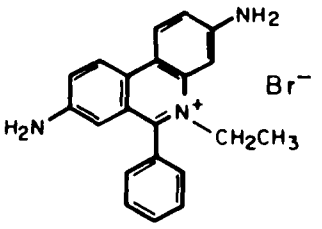


Ethidium Bromide

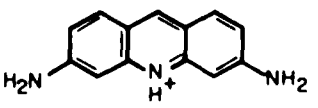


Proflavine

**Figure 1** Structures of EB and PF.

absorbance measured with the polarization vector parallel ($A_{\parallel}$) or perpendicular ($A_{\perp}$) with respect to the direction of flow. The LD signals are a function of (1) the orientations of the transition moments with respect to the flow direction, and can therefore be either positive or negative in sign, (2) the absorption spectra of the oriented species, and (3) the degree of orientation of the macromolecules in the flowing solution. The sign of the LD signal in the absorption region of the DNA (230–300 nm) is negative in sign for both linear[15] and supercoiled[14] DNA.

For the LD experiments, the DNA samples ($7.5 \times 10^{-5}$ *M*) were dissolved in 5 m*M* Tris buffer containing 1 m*M* EDTA at pH 7.9, 24°C; each LD experiment requires about 1.2 mL of solution containing a minimum of 10 μg of DNA. The details of our LD apparatus are described elsewhere.[16] Here, we briefly describe only the homebuilt Couette cell used in these experiments. The radius of the inner rotating cylinder is $R_i$ = 1.10 cm, while that of the outer cylinder is $R_o$ = 1.15 cm (annular gap = 0.05 cm). The inner cylinder was filled with fresh doubly distilled water, and rotated at speeds of up to 1300 rpm. The velocity gradient $G$ was calculated from the formula[17]

$$G(s^{-1}) = \frac{2\pi RV}{(R_o - R_i)} \qquad (2)$$

where $R$ is the mean radius [$R = (R_o + R_i)/2$], and the rotation speed $V$ of the inner cylinder is given in revolutions per second. The velocity gradient in all experiments, unless otherwise noted, was 1840 $s^{-1}$. These gradients were well below the rates required for shear degradation of linear DNA molecules.[18] Indeed, subjecting the supercoiled DNA (or the sonicated calf thymus DNA) to the hydrodynamic forces in a Couette cell operating at $V$ = 15 $s^{-1}$ for at least 30 m did not cause any measurable changes in the LD signals at 258 nm.

Theoretical considerations suggest that the critical velocity gradient $G_c$, corresponding to the maximum rotation speed at which laminar flow characteristics should still be observed, is equal to[19,20]

$$G_c = \frac{\pi^2}{(0.057)^{1/2}} \times \frac{\rho}{\eta} \times \frac{(R)^{1/2}}{(R_o - R_i)^{5/2}} \qquad (3)$$

where $\rho$ and $\eta$ are the density and the viscosity of the solution, respectively. For $G > G_c$ = 800 $s^{-1}$ ($G_c$ calculated using the dimensions of our Couette cell), Taylor instabilities[19] are expected to set in and the flow is expected to be nonlaminar. However, the LD signals increase smoothly with increasing $G$ up to $G$ values of at least 3000 $s^{-1}$ (see below), a fact that has been noted previously in the case of linear DNA.[15,21,22] Possible reasons for the apparent absence of nonlaminar flow effects at flow gradients above $G_c$ have been briefly discussed by Lee and Davidson.[17]

In order to follow the changes in conformation of supercoiled DNA as a function of EB (or PF) concentration, small aliquots of concentrated aqueous solutions of the drugs were successfully injected into the DNA solutions, and the LD spectra were scanned after each injection from 240 to 580 nm in the case of EB, or 240 nm to 500 nm in the case of PF. The maximum volume change due to the injection of the concentrated EB solutions was at most 1.5%; these small volume changes were neglected. The monochromator scanning rate was 120 nm/m, and the response time of the signal lock-in amplifier was fixed at 300 ms in order to increase the signal/noise ratio. The concentrations of EB and PF were calculated from the known molar extinction coefficients of both drugs in the absence of DNA (5800 $M^{-1}$ $cm^{-1}$ for EB at 480 nm, and 34,500 $M^{-1}$ $cm^{-1}$ for PF at 445 nm).

## RESULTS

### Absolute Reduced LD

Typical LD signals of linear and of supercoiled DNA as a function of the velocity gradient are shown in Figure 2. The LD signals are expressed in terms of the output voltage of the lock-in signal amplifier. However, the absolute response of the apparatus was also calibrated utilizing crossed polarizers. The absolute or reduced linear dichroism LD/A, where A is the absorbance of the DNA samples at 258 nm, is about −0.14 in the case of unsonicated calf thymus DNA at $G$ = 3000 $s^{-1}$. This value of LD/A is similar to the values given by other workers for native double-stranded DNA.[15,23] The LD signal of the supercoiled DNA is about five times smaller under identical experimental conditions, and thus the characteristic LD/A values are only −0.03 at $G$ = 3000 $s^{-1}$; this is an upper limit for the RF I supercoiled form, since the samples are always contaminated with nicked RF II DNA. The LD signals due to nicked circular DNA[14] or linear DNA are higher than those of supercoiled DNA.

The photosensitization of the DNA-bound drug

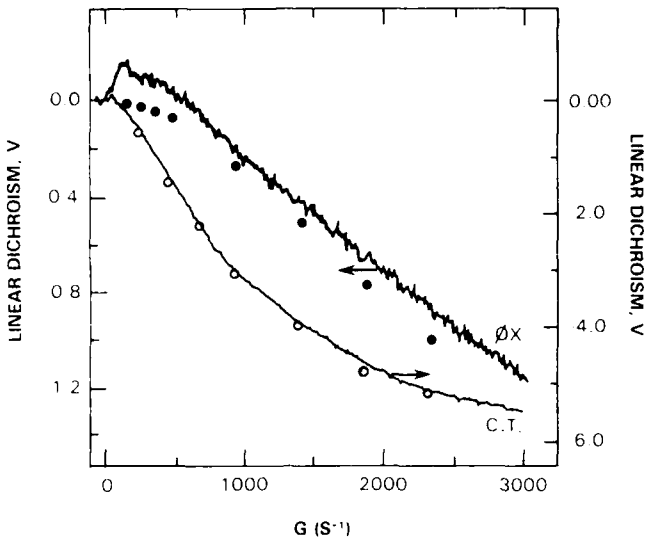


**Figure 2** Relative LD signals at 258 nm (arbitrarily expressed in units of volts) of supercoiled ($\phi$X 174) and calf thymus (C.T.) DNA as a function of the velocity gradient $G$. Continuous lines: the velocity gradient was increased from zero to the maximum value at a constant rate of 750 $s^{-2}$; (○) calf thymus DNA, (●) supercoiled DNA: the flow gradient was allowed to reach a preselected value and the LD signal was measured 60 s later. DNA concentration: $7.5 \times 10^{-5}$ $M$.

molecules can, in principle, lead to single-strand breaks resulting in a complete relaxation of the supercoiled DNA. It was therefore verified that there were no measurable changes in the ratio of (supercoiled)/(nicked) DNA molecules during the LD experiments by both gel electrophoresis and the LD technique. Simulating the experimental illumination (and rotation) conditions even at the higher EB concentrations used in these experiments, there were no detectable changes in the ratios of (supercoiled)/(nicked) molecules detectable by the gel electrophoresis assays. As is shown below, the magnitude of the LD signal at 260 nm changes by a factor of greater than three upon complete unwinding of the supercoiled DNA; nevertheless, subjecting the EB-DNA samples to the experimental conditions of the Couette cell (including illumination) at constant EB concentrations did not cause any changes in the magnitude of the LD signals at 260 nm. Therefore, the extent of nicking of supercoiled DNA under our experimental conditions, if any, was negligible.

## Dependence of LD on Velocity Gradient $G$

The LD signals of the DNA at 258 nm in the absence of added drugs were measured in two different ways: (1) the rotation speed was increased at a constant rate, equivalent to a rate of increase in the velocity gradient $G/\Delta t = 750$ $s^{-2}$; and (2) the speed of rotation was allowed to reach a steady preselected value, and then the LD signal at 258 nm was measured about 60 s after equilibrium had been reached.

In the case of linear calf thymus DNA, the LD signals were identical when measured by either method (Figure 2). In the case of the supercoiled DNA there is a significant difference between the steady-state and continuous sweep LD values; at low $G$ values ($< 500$ $s^{-1}$), the LD signal is positive in sign in the continuous sweep case, and is close to zero in the steady-state case. Above $G = 1000$ $s^{-1}$ the magnitude of the LD signals is consistently higher in the steady-state case (closed circles) than in the continuous sweep case at all values of $G$ (Figure 2). Independent kinetic measurements show that the response time of the LD signal of supercoiled DNA is about 20–30 s (data not shown). In the case of linear DNA, the response time is less than the time required to change the rotation speed from one fixed value to another (about 5 s). The longer time response of supercoiled DNA suggests that some deformation of the molecule is occurring in the hydrodynamic force field, which leads to a better overall net alignment of the DNA bases with their planes tending to be tilted perpendicular to the flow lines.

At low values of $G$, the LD of supercoiled DNA is positive in sign, suggesting that at low velocity gradients the DNA bases have a weak net tendency

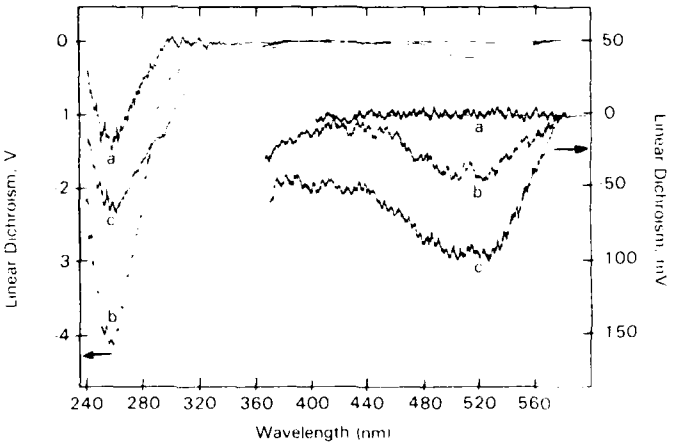


**Figure 3** LD spectra of EB-$\phi$X 174 DNA complexes at three different values of $r$ (moles drug added/mole nucleotide): (a) $r = 0.00$, (b) $r = 0.04$, and (c) $r = 0.10$. DNA concentration: $7.5 \times 10^{-5}$ $M$. LD scans were performed at a rate of sweep of 120 nm/m at a constant flow gradient ($G = 1840\ s^{-1}$).

of aligning with their planes parallel to the flow lines. A very weak initial positive LD signal at $G$ values below 60 $s^{-1}$ is also observed in the case of linear DNA. Norden and Seth reported that denatured DNA, in contrast to the double-stranded form, is characterized by positive LD spectra;[21] the small positive LD signals at low $G$ values therefore could be due to minor single-stranded regions present in the DNA molecules.

## LD Characteristics of EB- and PF-Supercoiled DNA Complexes

Typical LD spectra of $\phi$X 174 DNA without EB and at two different concentrations of EB ($r = 0.04$ and 0.10, where $r$ = moles drug molecules added/mole nucleotides) are shown in Figure 3. Within the DNA absorption band (below 300 nm), the LD signal due to $\phi$X 174 is negative in sign and resembles the absorption spectrum in shape, as in the case of linear DNA.[15,22,23] Above 400 nm, a weak negative LD signal due to EB molecules bound to the DNA is observed. As expected for intercalated drug molecules, the sign of this LD signal is negative.[23,27] Similar LD spectra at different ratios $r$ are shown for PF-$\phi$X 174 complexes in Figure 4; the negative LD band peaking at 462 nm coincides with the absorption band of PF bound to DNA[21,25] by an intercalation mechanism.[28]

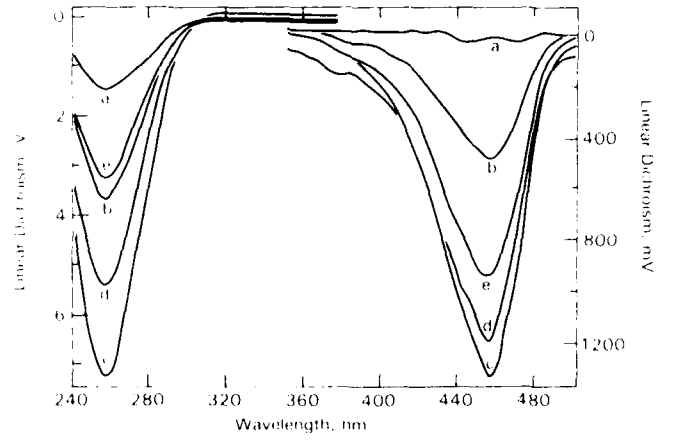


**Figure 4** LD spectra of PF-$\phi$X 174 complexes at different values of $r$: (a) $r = 0.00$, (b) $r = 0.04$, (c) $r = 0.05$, (d) $r = 0.06$, and (e) $r = 0.10$. Other conditions as in caption to Figure 3.

***EB–Supercoiled DNA Complexes.*** The reduced LD signal at 258 nm, which is predominantly due to the net overall orientation of the DNA bases, increases in magnitude by a factor of nearly 4 as $r$ is increased from zero to 0.04 by adding EB to either $\phi$X 174 DNA or SV40 DNA solutions; however, as $r$ is increased further to a value of 0.10, LD/A diminishes. The LD/A values at 520 nm due to bound EB molecules remain approximately constant in the region of $r$ (0.02–0.06) in which the LD/A ratio at 258 nm exhibits a pronounced minimum (Figure 5A and B). Below $r = 0.02$, the $(LD/A)_{258}$ ratios are rather uncertain because of the small LD signals and absorbance values.

The unexpected differences in $r$ dependence of the absolute LD in the 258- and 520-nm wavelength regions has also been observed in the case of pBR322 supercoiled DNA (data not shown). The LD signals at $r = 0$ and $r = 0.04$–$0.05$ correspond to supercoiled and completely unwound DNA, respectively (see below); typical ratios of LD signals, LD($r$ = 0.04–0.05)/LD($r$ = 0.00), were 3.7, 2.8, and 3.7 for $\phi$X 174, pBR322, and SV40 DNA, respectively.

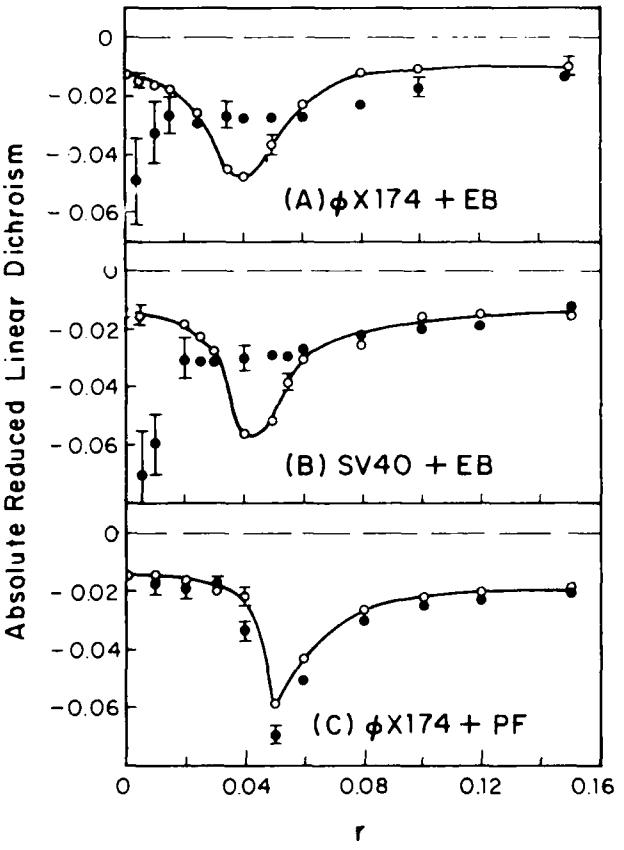


**Figure 5** Reduced LD (LD/A, in absolute units) at 258 nm (○, DNA absorption band) and within the bound drug absorption bands (●). (A) EB added to $\phi$X 174 supercoiled DNA, drug LD/A values determined at 520 nm; (B) EB added to SV40 supercoiled DNA, drug LD/A values determined at 520 nm; (C) PF added to $\phi$X 174 DNA, drug LD/A values determined at 462 nm. DNA concentration: $7.5 \times 10^{-5}$ $M$. Flow gradient: 1840 $s^{-1}$.

***PF–$\phi$X 174 DNA Complexes.*** The magnitude of the LD signal at 258 nm, for comparable values of $r$, is significantly larger in the case of PF than in the case of EB; also, the highest magnitude of the LD signal at 462 nm due to intercalated PF (at $r = 0.05$) is about 4.5 times greater than the analogous EB signal at 520 nm (at $r = 0.04$). These quantitative differences can be mostly attributed to the larger molar extinction coefficients of PF relative to those of EB. Because the magnitude of the LD signals is proportional to the absorbance of the intercalatively bound drug molecules, the influence of the drugs on the overall LD signals will be greatest at the absorption maxima of the drug molecules. According to measurements in our laboratory (data not shown), PF bound to DNA is characterized by maxima at 256 (molar extinction coefficient $\epsilon = 29{,}300\ M^{-1}\ cm^{-1}$) and 462 nm ($\epsilon = 32{,}700$), while the absorption maxima of EB bound to DNA are located at 298 ($\epsilon$ = 27,600) and 520 nm ($\epsilon = 4100$); this latter value is in good agreement with the results of Houssier et al.[25] Thus the absorption and LD spectra of intercalated PF molecules nearly coincide below 300 nm with those of the DNA bases, and the overall LD signal near 258 nm is thus greater than in the case of EB–DNA complexes; in the latter case, the absorption maximum of intercalated EB at 296 nm manifests itself as a shoulder in the LD spectra near 300 nm (Figure 3).

The reduced LD values at 258 and 462 nm as a function of $r$ for PF–$\phi$X 174 DNA complexes are shown in Figure 5C. These two curves resemble one another in shape, both reaching minima at $r = 0.05$. These results indicate that the PF molecules and DNA bases exhibit similar degrees of orientation in these flow gradient LD experiments, as expected in a simple intercalation model.

## LD Characteristics of Drug–Linear DNA Complexes

The reduced LD values of EB- and PF–calf thymus DNA complexes as a function of $r$ within the DNA and drug absorption bands are shown in Figure 6. In contrast to the behavior of supercoiled DNA at similar values of $r$, the LD/A values at 258 nm and within the absorption bands of the complexed drug molecules are nearly constant as a function of added drug concentration. The slight increase at the higher

$r$ values may reflect the stiffening of the DNA segments due to the intercalative binding of the drug molecules; the reduced LD values at 258 and at 462 nm are nearly identical in the case of PF, as expected for classical intercalation complexes.[26] The small differences between the $(LD/A)_{258}$ and $(LD/A)_{520}$ values in the case of EB have been reported earlier by others as discussed in the review of Houssier.[26]

The results obtained with the sonicated linear DNA–drug complexes show that the LD signals as a function of r obtained with supercoiled DNA are not due to artifacts of the Couette cell measurements.

## DISCUSSION

### Correlations Between Magnitude of LD, Sedimentation Coefficients, and Changes in Superhelical Density

***The Effects of Drug Concentration.*** In Waring's paper,[6] the sedimentation coefficients ($S_{20}$) are plotted as a function of $\nu_c$, the ratio of *bound* drug molecules per nucleotide. Our LD results are plotted as a function of $r$, the concentration of *added* drug molecules per DNA nucleotide. However, we performed equilibrium dialysis measurements at $r = 0.05$ and found that under our experimental conditions more than 95% of the drug molecules are bound to the DNA (data not shown); this is consistent with previous results of Crawford and Waring[29] in the case of EB, and the known high association constants ($\sim 10^6\ M^{-1}$) of EB[25] and PF[30] measured at relatively low ionic strengths, similar to those employed in our experiments. Thus, $r = \nu_c$ (for $r < 0.1$); this is confirmed by comparing our values of $r$ corresponding to the minima in the LD/A curves, with the values of $\nu_c$ corresponding to the minima in the $S_{20}$ coefficients in Waring's experiments.[6] These minima correspond to the "equivalence point," where the sedimentation coefficients are the same at this value of $\nu_c$ for nicked and for the fully relaxed $\phi$X 174 DNA forms.[6]

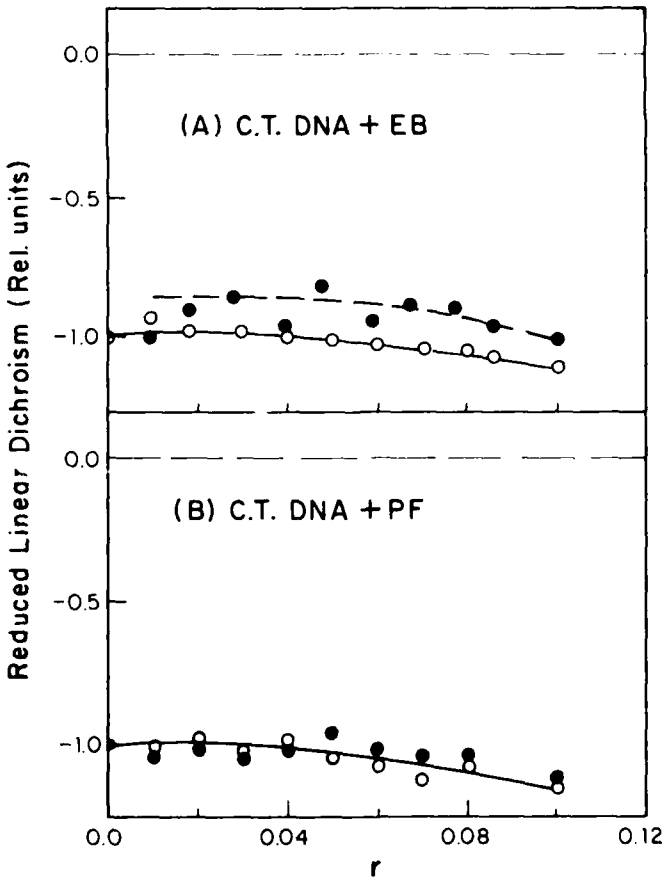




**Figure 6** Reduced LD values (in relative units) of EB- and PF-sonicated calf thymus DNA complexes. (A) EB (●, measured at 520 nm), and (B) PF (●, measured at 462 nm); (○) LD/A values determined at 258 nm. DNA concentration: $7.5 \times 10^{-5}\ M$; flow gradient: $1840\ s^{-1}$.

***The Equivalence Point and Unwinding Angles.*** The equivalence point in our experiments is reached at $r = 0.04 \pm 0.005$ in the case of EB–$\phi$X 174 DNA complexes (Figure 5A). In Waring's sedimentation experiments, the equivalence point was reached at $\nu_e = 0.04$.[6] In the case of PF and $\phi$X 174 DNA, our equivalence point occurs at $r = 0.05 \pm 0.005$, whereas in Waring's sedimentation coefficient experiments the equivalence point lies in the range of $\nu_e = 0.045$–0.065, again suggesting that $r$ and $\nu_e$ are very close to one another, as indicated also by the experiments of Ramstein et al.[27] for values of $r < 0.1$.

The differences in the $\nu_e$ values at the equivalence points have been attributed to differences in the unwinding angles $\theta$ per bound drug molecule.[1,6] In the case of EB,[2,7,31] the accepted value for $\theta$ is 26°, while for PF[31] $\theta = 17°$. When the superhelix density $\sigma$ (number of superturns/10 base pairs) is known, the unwinding angle $\theta$ can be calculated from $\nu_e$ according to the equation[1,2]

$$\theta = (-180\sigma/\nu_e) \qquad (4)$$

The superhelix density of $\phi$X 174 is −0.057[1]; using the values of $r$ deduced from the LD/A minima in Figure 5, $\theta$ values of $26 \pm 2°$ and $21 \pm 2°$ are obtained for EB and PF, respectively. The latter value is slightly larger than the one given in the literature.[2]

The results shown in Figure 5A and B, as well as similar results obtained with pBR322 DNA (results not shown), suggest that the LD technique is suitable for following the unwinding of different kinds of supercoiled DNA by EB. In all cases, the same biphasic behavior of the LD signal as a function of $r$ is observed. However, the equivalence point appears at slightly higher values of $r$ in the cases of pBR322 ($r = 0.05$) and SV40 DNA. The superhelical density of the latter is the same as that of $\phi$X 174[1]; the number of base pairs per $\phi$X 174,[32,33] pBR322,[34] and SV40[35,36] molecule, is 5386, 4363, and 5243, respectively. From the sequences provided in the cited references, we estimate that the GC content is 46, 54, and 41%, respectively. Therefore, these factors cannot account for the observed differences in the observed $r$ ratios at the equivalence points. Other, more trivial effects such as heterogeneities in superhelical densities,[2] contamination of the samples with nicked and linear forms, can also play a role in determining the apparent values of $\nu_e$.

***The Shapes of the Titration Curves.*** The dependence of the $(LD/A)_{258}$ values of supercoiled $\phi$X 174 DNA as a function of EB and PF concentrations is remarkably similar to the sedimentation coefficient curves published earlier by Waring.[6] The increase in the magnitude of the LD signal as $r$ is increased from zero to about 0.04–0.05 is attributed to a drug-induced unwinding of supercoiled DNA, which causes a decrease in the $S_{20}$ coefficient[6] and an increase in the magnitude of the LD signal at 258 nm. Partially or fully unwound forms of $\phi$X 174 DNA exhibit a greater LD signal due to their larger, more extended hydrodynamic shapes, in contrast to supercoiled DNA, which is characterized by smaller LD values (or higher $S_{20}$ coefficients). At an $r$ value near 0.04, all superturns are removed, giving the DNA molecules an untwisted open circular topology, a state characterized by $\sigma = 0$. In the case of proflavine, this state is reached at a slightly higher value of $r = 0.05$. At still higher $r$ values, left-handed superturns, corresponding to a positive increase in the superhelical density, are introduced as a result of the binding of the drug molecules; this results in a more compact form (lower LD values) and greater $S_{20}$ coefficients.

The LD/A curves are rather symmetrical in the case of EB (Figure 5A and B). In the case of proflavine (Figure 5C), the LD/A signal as a function of $r$, after passing through the minimum, does not return to its initial value as $r$ is increased further. A similar asymmetry was noted by Waring in his $S_{20}$ vs $\nu_e$ curves.[6] The reasons for such asymmetric titration curves have been discussed by Bauer and Vinograd.[1] These reasons include the following: (1) the relative binding affinity of EB (and probably other intercalating drug molecules) depends on the superhelical density, favoring supercoiled forms at $\nu < \nu_e$, and linear DNA forms at $\nu > \nu_e$; (2) the degree of asymmetry depends on the initial values of the superhelical density, and the maximum number of intercalated drug EB molecules that can bind to the DNA at values of $r > 0.1$; it may be difficult to achieve a sufficiently high binding level to rewind the DNA in a positive sense to achieve the same original magnitude of $|\sigma|$.

## Tertiary Structure and Contributions of DNA Bases and Drug Molecules to the LD Signals Measured at Different Wavelengths

The characteristics of linear DNA in a hydrodynamic flow gradient have been considered by a number of different authors. Wada[22] and Nordén and Tjerneld[23] approximated the behavior of DNA in terms of the Peterlin–Stuart theory[37] for rigid ellipsoids of revolution; deviations from this theory due to the deformation and extension of the DNA molecules in the hydrodynamic flow field were also

considered by Nordén and Tjerneld.[23] Shimada and Yamakawa[38] derived a theoretical treatment for hydrodynamic orientation of polymers based on the worm-like coil model; Schellman and co-workers used the bead-spring model for descriptions of the polymer chains.[39,40] In both of these models, the flexibility and deformation of DNA molecules in the hydrodynamic flow is taken into account. Overall, the DNA molecules may be viewed as a series of linked, relatively stiff segments that become partially oriented with their axes tending to align themselves parallel to the flow lines, thus accounting for the observed negative LD signals within the DNA absorption band.

Some elements of these models, particularly deformation and partial alignment of DNA segments along the flow lines, may also be applicable to covalently closed circular DNA. However, the closed circular nature of the intertwined DNA strands imposes restrictions on the overall degree of orientation of the individual DNA segments in the hydrodynamic force field.

Superimposed on these effects is the change in the overall hydrodynamic shape and size of the DNA molecules due to the changes in superhelicity induced by the binding of drug molecules. The lower the superhelicity, the greater the apparent hydrodynamic size of the molecules,[1-13] and thus the smaller the overall Brownian rotational motions of the DNA molecules. Therefore, unwinding should be accompanied by a better overall alignment of these molecules along the flow lines in the Couette cell. This effect, independent of any motion of the individual segments, is believed to account for the higher magnitudes of LD signals at the equivalence point relative to the LD signals of the highly compact supercoiled forms. Intuitively, it appears evident that the overall orientations of such segments in the flow field will be lower in the highly twisted supercoiled forms, than in the relaxed or linear DNA forms.

The seemingly anomalous difference in the $r$ dependencies of the $(LD/A)_{258}$ and $LD_{520}$ signals suggests that the unwound DNA segments containing EB molecules may respond differently to the hydrodynamic force field than the closed circular DNA molecule as a whole, or than DNA segments containing few or no EB molecules. At values of $r$ beyond the equivalence point, ethidium molecules are known to bind preferentially to linear rather than to supercoiled DNA[1]; thus the distribution of EB molecules within any single closed circular DNA molecule may be quite heterogeneous, accounting for differences in the response of different regions of the DNA molecules to the hydrodynamic forces tending to align these segments. Any one of these effects, or a combination thereof, could account for the differences in the $r$ dependencies of the LD signals at 258 nm and at 520 nm in the case of the EB-supercoiled DNA complexes.

It is evident that the behavior of the LD signals of the PF molecules as a function of $r$ more closely parallel the LD signal at 258 nm than the analogous EB LD signals; the variations in the LD signals at 258 nm as a function of $r$ are ascribed to the changes in the overall size of the DNA molecules, differences in deformation of the tertiary structure, and the partial alignment of DNA segments along the flow lines. While the exact reasons for these differences in behavior between EB- and PF-supercoiled DNA complexes are not known, these differences may be related to the known differences in the binding geometries of these two drug molecules. As established by other workers,[16,23,27] PF is characterized by an orientation angle $\theta = 90°$ (orientation of in-plane transition moment of the drug molecules with respect to the axis of B-form DNA), as expected for classical intercalation complexes. On the other hand, the transition moments of the EB molecules appear to be tilted with respect to the planes of the DNA bases[25,26,29,41] ($\theta = 60°-75°$), which suggests that the binding geometry may be somewhat different than in the case of PF. Furthermore, different intercalators may affect the local torsional rigidities and dynamics of supercoiled DNA to different extents,[42] which in turn may affect the deformation of the DNA molecules and/or the alignment of individual DNA segments. In addition, there may be differences in the binding affinities of PF and EB to DNA of different superhelical densities.

## CONCLUSIONS

The flow LD technique is a suitable hydrodynamic method for rapidly assaying variations in the properties of supercoiled DNA induced by the binding of drug molecules. The conformational properties of the bound drug molecules causing these changes can also be monitored. The 258-nm LD signal reflects the overall shape and hydrodynamic properties of the partially supercoiled DNA molecules, while the 520-nm LD signals due to bound EB molecules may reflect the partial alignment of individual DNA segments containing the bound drug molecules. In contrast, the reduced LD values due to the supercoiled DNA bases at 258 nm and due to complexed PF molecules at 462 nm appear to more closely reflect

analogous degrees of alignment of both moieties in the flow gradients, as expected for a simple intercalation model of binding.

This work was supported by the Department of Energy at the Radiation and Solid State Laboratory at New York University, Grant No. DE-FG02-86ER60405). We thank Dr. Y. Mnyukh for performing the LD experiments, and B. Mao and S. Birke for their assistance in some of the other experiments.

## REFERENCES

1. Bauer, W. & Vinograd, J. (1974) in *Basic Principles in Nucleic Acid Chemistry*, Vol. II, Ts'o, P. O. P., Ed., Academic Press, New York, pp. 265–303.
2. Bauer, W. R. (1978) *Ann. Rev. Biophys. Bioeng.* **7,** 287–313.
3. Scovell, W. M. (1986) *J. Chem. Ed.* **63,** 562–565.
4. Sinden, R. R. (1987) *J. Chem. Ed.* **64,** 294–301.
5. Bauer, W. & Vinograd, J. (1968) *J. Mol. Biol.* **33,** 141–171.
6. Waring, J. (1970) *J. Mol. Biol.* **54,** 247–279.
7. Wang, J. C. (1974) *J. Mol. Biol.* **89,** 783–801.
8. Pulleyblank, D. E. & Morgan, A. R. (1975) *J. Mol. Biol.* **91,** 1–13.
9. Keller, W. (1975) *Proc. Nat. Acad. Sci. USA* **72,** 4876–4880.
10. Liu, L. F. & Wang, J. C. (1975) *Biochim. Biophys. Acta* **395,** 405–412.
11. Espejo, R. T. & Lebowitz, J. (1976) *Anal. Biochem.* **72,** 95–103.
12. Revet, B. M. J., Schmir, M. & Vinograd, J. (1971) *Nature New Biol.* **229,** 10–13.
13. Smit, E. M. & Borst, P. (1971) *FEBS Lett.* **14,** 125–129.
14. Yoshida, H., Swenberg, C. E. & Geacintov, N. E. (1987) *Biochemistry (USA)* **26,** 1351–1358.
15. Wada, A. & Kozawa, S. (1964) *J. Polym. Sci.* **2,** 853–864.
16. Geacintov, N. E., Ibanez, V., Rougee, M. & Bensasson, R. V. (1987) *Biochemistry (USA)* **26,** 3087–3092.
17. Lee, C. S. & Davidson, N. (1968) *Biopolymers* **6,** 531–550.
18. Davison, P. F. (1959) *Proc. Natl. Acad. Sci. USA* **45,** 1560–1568.
19. Taylor, G. I. (1923) *Phil. Trans.* **A223,** 289–343.
20. Jerrard, H. G. (1950) *J. Appl. Phys.* **21,** 1007–1013.
21. Nordén, B. & Seth, S. (1979) *Biopolymers* **18,** 2323–2339.
22. Wada, A. (1964) *Biopolymers* **2,** 361–380.
23. Nordén, B. & Tjerneld, F. (1976) *Biophys. Chem.* **4,** 191–198.
24. Houssier, C. & Kuball, H.-G. (1971) *Biopolymers* **10,** 2421–2433.
25. Houssier, C., Hardy, B. & Fredericq, E. (1974) *Biopolymers* **13,** 1141–1160.
26. Houssier, C. (1981) in *Molecular Electrooptics*, Krause, S., Ed., Plenum, New York, pp. 313–398.
27. Ramstein, J., Houssier, C. & Leng, M. (1973) *Biochim. Biophys. Acta* **335,** 54–68.
28. Neidle, S., Pearl, L. H., Herzyk, P. & Berman, H. M. (1988) *Nucleic Acids Res.* **16,** 8999–9016.
29. Crawford, L. V. & Waring, M. J. (1967) *J. Mol. Biol.* **25,** 23–30.
30. Ellerton, N. F. (1969) *Biopolymers* **8,** 767–786.
31. Waring, M. J. (1981) *Ann. Rev. Biochem.* **50,** 159–192.
32. Sanger, F., Air, G. M., Barrell, B. G., Brown, N. L., Coulson, A. R., Fiddes, J. C., Hutchinson, C. A., III, Slocombe, P. M. & Smith, M. (1977) *Nature* **265,** 687–695.
33. Sanger, F., Coulson, A. R., Friedman, T., Air, G. M., Barrell, B. G., Brown, N. L., Fiddes, J. G., Hutchinson, III, C. A., Slocombe, P. A. & Smith, M. (1978) *J. Mol. Biol.* **125,** 225–246.
34. Maniantis, J., Fritsch, E. F. & Sambrook, J. (1982) in *Molecular Cloning: a Laboratory Manual*, Appendix B, Cold Spring Harbor Laboratory, New York, pp. 479–487.
35. Reddy, V. B., Thimmappaya, B., Dahr, R., Subramanian, K. N., Zain, B. S., Pan, J., Ghosh, P. K., Celma, M. L. & Weissman, S. M. (1978) *Science* **200,** 494–502.
36. Fiers, W., Contreras, R., Haegeman, C., Rogiers, R., van de Voorde, A., Van der Heuverswyn, H., Von Herreweghe, J., Volckaert, G. & Ysebaert, M. (1978) *Nature* **273,** 113–120.
37. Peterlin, A. & Stuart H. A. (1939) *Z. Physik* **112,** 1–19.
38. Shimada, J. & Yamakawa, H. (1976) *Macromolecules* **9,** 583–586.
39. Wilson, R. W. & Schellman, J. A. (1977) *Biopolymers* **16,** 2143–2165.
40. Schellman, J. A. (1980) *Biophys. Chem.* **11,** 321–328.
41. Hogan, M., Dattagupta, N. & Crothers, D. M. (1979) *Biochemistry (USA)* **18,** 280–288.
42. Wu, P., Song, L., Clendenning, J. B., Fujimoto, B. S., Benight, A. S. & Schurr, J. M. (1988) *Biochemistry* **27,** 8128–8144.

*Received June 21, 1989*
*Accepted January 3, 1990*